

# The SED Machine - A Dedicated Transient IFU Spectrograph

Sagi Ben-Ami<sup>a</sup>, Nick Konidaris (PI\*)<sup>b</sup>, Robert Quimby (PS†)<sup>c</sup>, Jack T.C Davis<sup>b</sup>, Chow Choong Ngeow<sup>d</sup>, Andreas Ritter<sup>d</sup>, Alexander Rudy<sup>d</sup>

<sup>a</sup> Department of Particle Physics and Astrophysics, The Weizmann Institute of Science, Rehovot 76100, Israel.

<sup>b</sup> Cahill Center for Astronomy and Astrophysics, California Institute of Technology, 1200 E California Blvd., Pasadena, CA 91125, USA.

<sup>c</sup> Kavli-IPMU, University of Tokyo, Kashiwanoha 5-1-5, Kashiwa-shi, Chiba, Japan.

<sup>d</sup> Graduate Institute of Astronomy, National Central University, Jhongli City, 32001, Taiwan.

## ABSTRACT

The Spectral Energy Distribution (SED) Machine is an Integral Field Unit (IFU) spectrograph designed specifically to classify transients. It is comprised of two subsystems. A lenselet based IFU, with a  $26'' \times 26''$  Field of View (FoV) and  $\sim 0.75''$  spaxels feeds a constant resolution ( $R \sim 100$ ) triple-prism. The dispersed rays are then imaged onto an off-the-shelf CCD detector. The second subsystem, the Rainbow Camera (RC), is a 4-band seeing-limited imager with a  $12.5' \times 12.5'$  FoV around the IFU that will allow real time spectrophotometric calibrations with a  $\sim 5\%$  accuracy. Data from both subsystems will be processed in real time using a dedicated reduction pipeline. The SED Machine will be mounted on the Palomar 60-inch robotic telescope (P60), covers a wavelength range of 370 – 920nm at high throughput and will classify transients from on-going and future surveys at a high rate. This will provide good statistics for common types of transients, and a better ability to discover and study rare and exotic ones. We present the science cases, optical design, and data reduction strategy of the SED Machine. The SED machine is currently being constructed at the Calofornia Institute of Technology, and will be comissioned on the spring of 2013.

## 1. SCIENCE CASE

According to the Astro-2010 decadal report, the field of time-domain astronomy is expected to enjoy a golden age during this decade. The number of on-going and soon-to-be-commissioned optical surveys, such as PTF<sup>‡</sup>, PanSTARRS<sup>§</sup>, CSS<sup>¶</sup>, SkyMapper<sup>||</sup>, as well as the Large Synoptic Survey Telescope (LSST<sup>1</sup>), to be commissioned in 8 – 10years, are and will keep this field vibrant well into the next decade.

Traditionally, classification of explosive transients is done mainly by spectral observations of the transients using medium to large aperture telescopes. However, even with a relatively large amount of telescope time allocated for spectral classification and follow-up, current sky surveys are struggling to keep up with the discovery rate. Since the rate of transient discoveries from future surveys is expected to rise, a new approach must be taken. The SED Machine, a low resolution ( $R = \frac{\lambda}{\Delta\lambda} \sim 100$ ) spectrograph designed for the class of 1m–3m telescopes, offers a novel approach for explosive transient classification. The SED Machine key scientific objectives are:

- Spectroscopy of infant supernovae - early time data can provide powerful clues to the origins and physics of supernovae of all types. As can be seen in figure 1, a resolution of  $R \sim 100$  contains as much information for classification as spectra at  $R \sim 1000$ , but with more than  $3\times$  increase in signal to noise per second.
- Shock breakout - the SED Machine will produce a broad band synthetic spectrum with an accuracy of 5%. This will be helpful to identify shock breakout of type II supernovae, that carry valuable information about the SN progenitors and explosion physics<sup>2</sup>.

---

Principal Investigator

Project Scientist

<sup>‡</sup>Palomar Transient Factory (<http://www.astro.caltech.edu/ptf/>)

<sup>§</sup><http://pan-starrs.ifa.hawaii.edu/public/>

<sup>¶</sup>Catalina Sky Survey (<http://www.lpl.arizona.edu/css/>)

<sup>||</sup><http://msowww.anu.edu.au/skymapper/>

- Rare Supernovae - The SED Machine has the ability to sort through the mundane optical transients and discover the more rare phenomena, such as superluminous supernovae, and gap objects in the nearby universe<sup>3,4</sup>.
- GRBs - the SED can function as a low-resolution photometric redshift instrument<sup>5,6</sup>, providing prompt redshift for GRBs in the redshift range of  $z \approx 2 - 6$ .
- Asteroids - Spectroscopic observations inform us of the current physical properties and chemical compositions of the asteroid surface. The SED Machine is very well suited to classification of asteroids, as the taxonomy of Bus & Binzel<sup>7</sup> is itself based on  $R \sim 100$  optical spectroscopy.

## 2. THE INSTRUMENT

The SED Machine will be mounted on the Palomar 60-inch telescope. Figure 2 shows the optical interfaces of the SED Machine from the P60 focal plane to the image plane of each subsystem.

The IFU has a  $\sim 26'' \times 26''$  FoV divided in hexagonal spaxels. The dispersing element of the spectrograph is a constant resolution prism, custom manufactured by JENOPTIK Optical Systems, Inc. The detector package for the IFU spectrograph is a PIXIS 2048-Excelon camera from Princeton Instruments. The Rainbow Camera (RC) is a  $12.5' \times 12.5'$  imager with a FoV divided to 4 different bands - Sloan  $u, g, r, i$ . Photometric data from bright stars in the RC FoV will be compared to star catalogs, allowing spectrophotometric calibration of the spectra simultaneously recorded by the IFU within an accuracy of 5%. In the following sections we describe the IFU spectrograph, and RC in depth.

### 2.1 IFU Spectrograph

We divide the IFU spectrograph to three parts: (i) a magnifier/expander reimages the telescope focal plane onto the lenslet array. (ii) a lenslet array is focused on the telescope primary mirror and produces a set of telescope pupil images. (iii) a standard spectrograph dispersing pupil images, comprised from a collimator, a prism, and a camera. The paraxial layout of the IFU spectrograph is given in figure 3.

The Palomar 60-inch telescope operates at  $f/8.75$  and thus has a plate scale of  $65\mu\text{m}$ . The fore optics magnifies the telescope field by about  $10.5\times$  onto an hexagonal lenslet array of  $0.444\text{mm}$  pitch so that each spaxel subtends a  $\sim 0.64''$  field. The spaxel size was chosen so that it maximizes signal to noise ratio, considering field-of-view and typical seeing tradeoffs.

Through the foreoptics the lenslet array is focused on the P60 primary mirror. Its purpose is to slice up the field and produce an array of telescope images.<sup>8</sup> The each lens in the array operates at  $f/4.5$  with an effective focal length of  $2.26\text{mm}$ . It is manufactured by Advanced Microoptical Systems in Germany and is made of fused silica, care was taken to design an array with a high fill factor, and laboratory verification of delivered arrays is ongoing.

After the array of pupil images is formed, the SED Machine is a standard spectrograph. The pupil images are magnified by about  $\sim 1.3\times$  through the collimator/camera pair with a beam size of  $\sim 30\text{ mm}$ . The lenses were designed by Nick Konidaris with zemax. The 80 percent ensquared energy sizes are predicted to be less than 2 pixels at all wavelengths and field positions. Lateral color is controlled such that the spectra are easily separable over 95% of the field. Normally lateral color is ignore in spectrograph cameras, but here has to be well controlled as the blue end of one spectrum is next to the red end of another.

### 2.2 Rainbow Camera

The RC is an imager subsystem taking images at four bands simultaneously: Sloan  $u, g, r$ , and  $i$ . Photometric reduction of the obtained images will be used to correct for atmospheric extinction, seeing variations, and other time dependent factors that affect the system transmittance. As a concept, the RC is derived from the system used by the SNIFS spectrograph.<sup>9</sup> The RC will also function as the instrument guider, taking images of the transient surrounding field of view every minute. Bright stars from the RC Full Field of View (FFoV) will be used to guide and position the IFU spectrograph on the transient during each exposure.

The SED Machine RC was designed using Zemax, a commercial program for optical system design. In our design approach we tried to use off-the-shelf lenses whenever possible, incorporating two custom lenses into the system.

The system operates at  $f/4.8$ , with an effective focal length  $f = 89.7\text{mm}$ , and a  $12.5' \times 12.5'$  FoV, giving a scale of  $35.9\mu\text{m}/\text{arcsec}$ . The basic characteristics of the system are given in table 1, and the system layout is given in figure 4. The RC performance plot is shown in figure 5. Average spot diameter and spot diameter variance are

$f/\#$	4.8
EFL	89.7mm
Pixel scale	$0.375''$
FFoV	$12.5' \times 12.5'$
Paraxial magnification	0.56
Total track	368.9mm
Detector size	$27.7\text{mm}^2$

Table 1. RC optical characteristics. Data is calculated for  $\lambda = 505\text{nm}$ .

$u = 0.65'' \pm 0.07''$ ,  $g = 0.51'' \pm 0.3''$ ,  $r = 0.6'' \pm 0.13''$ ,  $i = 0.5'' \pm 0.2''$ , all below the seeing at the P60 telescope. The RC is free of vignetting up to an angular distance of  $6.6'$  from the optical axis, falling by 5% at the axial edge of the FoV. The total transmittance, assuming a quarter-wavelength AR coating of MgF2 for the achromat triplet, and a 99% AR coating for the other elements, is given in figure 5 and is  $\sim 75\%$  for all wavelengths of operation.

As part of the design process, we have done a tolerance, thermal, and ghost analysis. The proposed system has shown a deviation of less than  $0.3''$  in spot diameter for all fields, at all expected operating temperature, and when allowing reasonable deviations in positioning and alignment, and when considering fabrication tolerances and material imperfections.

## 2.3 Optomechanical design

For the opto-mechanical design of the SED Machine there are two arms of the optical layout to consider, the IFU spectrograph and the Rainbow Camera. The system is shown in figure 6. The IFU spectrograph is the more complex of the two in that there are more optics to be aligned as well as there being lens groups that must have optical axes aligned to within  $\sim 50\mu$ . The Rainbow Camera does have complexities as well but of the two it is definitely the simpler. Both arms of the optical layout originate in what we are calling the beam splitting structure. This is placed over the aperture where light from the telescope enters, and has a small prism to redirect a portion of the light perpendicularly into the IFU. The majority of the light continues as it came in, though a rainbow filter and into the Rainbow Camera optics.

**IFU Spectrograph:** Upon exit of the beam-splitting structure, there is an expander doublet held in delrin which is used to thermally stabilize the resulting picture on the detector with the same picture that goes through the rainbow camera. After the doublet there is a fold mirror that is used in order to maintain the beam over the breadboard. Then the beam enters a lenslet array that is mounted with 6 other optics in the collimator barrel. The barrel is held in a customized v-block that allows it to be taken out and replaced accurately. The beam then goes through a prism that is kinematically retained in its own customized housing. Upon exit of the prism it then goes into a camera barrel which is simpler than that of its collimator counterpart, but has its own complexities in that its v-block has to be able to translate along the optical beam by 1mm for focusing reasons. This was done by having the v-block be 2 parts, fixed and free, that are joined through the use of flexure stages and an actuator. Finally the beam enters a field flattener and into the detector.

**Rainbow Camera:** Upon exiting from the beam splitting structure, there is a series of optics that are being held by a cylinder of delrin. The purpose of this is to have these optics be thermally equivalent to the expander doublet in the IFU so as the temperature changes on a given day, both the IFU and the Rainbow Camera are both translating along the beam axis in the same vector, that is direction and magnitude. Upon exit from the delrin barrel there is a field flattener and the same detector as for the IFU.

## 3. USAGE OVERVIEW

As mentioned earlier, the SED machine will be mounted on the Palomar 60-inch robotic telescope.<sup>10,11</sup> It is the design team intention that the SED machine will be a fully automatic instrument, that will require

minimum intervention from end-users. The SED Machine will work as a complementary instrument to the Palomar Transient Factory survey (PTF). We envision the SED Machine will automatically take spectra of objects assigned to it through an interface to the PTF realtime transient detection system.<sup>12</sup> A description of the sequence of operation for a typical night follows.

After initial calibrations such as bias, flats, and arcs are taken during twilight time, science exposures will begin. The science target list will be comprised from  $\sim 20$  candidate transients and standard stars. The candidate transients are either: (i) new transients detected by the PTF assigned by humans or selected automatically based on pre-set thresholds-criteria, or (ii) unobserved targets from previous nights, or (iii) interesting targets that need additional follow-up observations. The integration time for each transient will be 20 minutes, divided to three sub-exposures. During the IFU exposure, the RC will take an image every minute that will be used for guiding, and spectrophotometric calibration. In each science exposure, Astrometry refinement will be performed on the first RC image, and relative positions between target and nearby reference stars will be calculated and used to make sure the science target falls within the IFU spectrograph field of view. At the end of each night calibration exposures will be repeated. At the end of each science exposure, data will be fed to a dedicated data reduction pipeline, described in the next section, where it will be reduced automatically.

#### 4. DATA REDUCTION

The data reduction pipeline (hereafter DRP) for the SED Machine is currently under development at the National Central University. The DRP will be responsible to process the raw data taken by the SED Machine to science grade products, and serves as the middle layer between the SED Machine scheduler and scientific analysis pipelines. The DRP consists of three major components: two reduction pipelines that will be run in parallel for the RC and the IFU, and an IFU Simulator for providing simulated IFU data when developing the IFU pipeline. In addition, several components are expected to be included in DRP, such as a database module for tracking the images, a data quality module for data quality measurements, and a data archive.

The simulator for SED Machine IFU (hereafter the Simulator) mathematically models the IFU spectrograph at  $R \sim 100$ , and creates an image that would be produced from the lenslet-based integral field spectrograph on the IFU detector. The Simulator models the source, as well as the throughput of the instrument and atmosphere, the geometric resampling due to the hexagonal lenslet array, and the dispersion across the image plane caused by the prism. The Simulator can also produce images from a variety of sources and under a variety of conditions (for examples, at a variety of temperatures and the effects of scattered light). The Simulator also handles flat, sky, bias and dark images for various instrument configurations. The Simulator will produce source-images from uniform sources mapped to a variety of positions on the CCD (see Figure 7). Further details of the Simulator will be presented in Rudy et al. (in preparation).

Preliminary design of the RC pipeline consists of a number of python scripts to reduce the RC images by using the pyRAF interface, and refining the astrometry for a given input RC image using algorithms from [astrometry.net](http://astrometry.net)<sup>13</sup>. At a later stage of the RC pipeline, reduced and astrometrically calibrated images will be stacked, followed by source detection and photometry using SExtractor<sup>14</sup>. Stellar fluxes in the RC images will be compared to published catalogs and the atmospheric extinction will be estimated. Extinction corrections will then be applied to the IFU spectra before they are delivered to PTF scientists.

The IFU reduction pipeline is based on the STELLA pipeline<sup>15</sup>. After bias subtraction, the apertures of a combined flat-field image are identified and traced. In order to remove the background for this procedure a reference scattered-light image is scaled to fit the background, and subtracted from the flat. Then, all pixels with values below a certain threshold are set to zero. Starting with the bottom row, the pipeline searches for the first signal which is wider than 2 FWHM of an assumed Gaussian spatial profile. The pipeline then traces the aperture by fitting Gaussian profiles for every row until the signal is lost. The traced aperture centers are fitted with a low-order polynomial, and the coefficients of the fit are saved to an aperture-definition file. The whole aperture is then set to zero and the procedure is repeated until all apertures have been identified and traced. For the scattered-light subtraction the Kriging algorithm<sup>16,17</sup> is utilized. The Kriging algorithm can be very expensive in terms of memory and computing time if a large number of samples (pixel values) is used. The IFU pipeline therefore looks for clusters on the CCD which only contain scattered light, and uses the median value of the cluster only for the center of the cluster. The CCD is then divided into a number of rectangular areas,

with the mean of all the clusters in each rectangle being assigned for the center of the rectangle. After scattered-light subtraction the object images are flat-fielded and extracted using a fast and stable re-implementation<sup>18</sup> of Piskunov's optimal-extraction algorithm<sup>19</sup>. During the extraction procedure cosmic rays are automatically identified and removed. After the wavelength calibration sky and background of the object of interest are calculated from the spectra surrounding the object and removed from the object spectra.

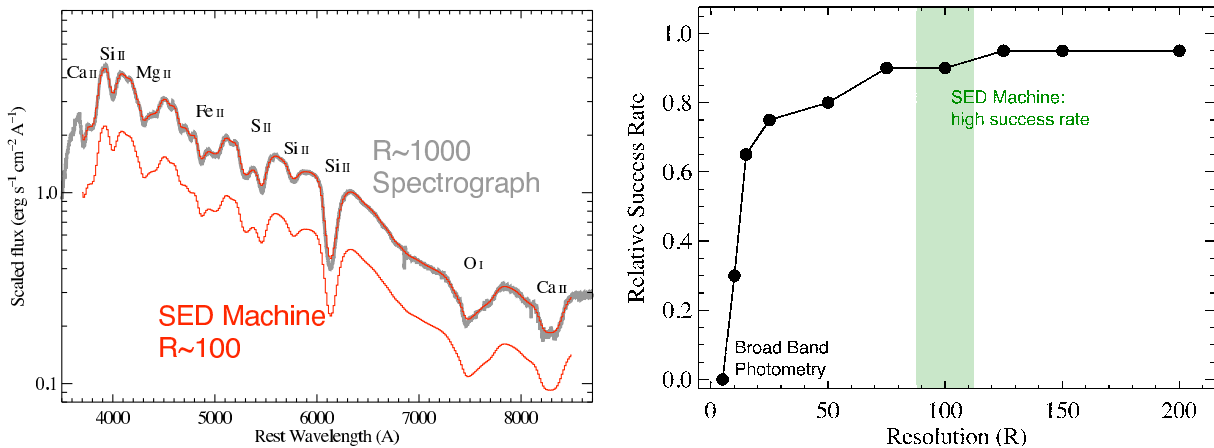


Figure 1. **Left:** Spectra of a type Ia supernova near maximum light at two resolutions:  $R \sim 1000$  (thick gray curve) and  $R = 100$  (thin red lines). Line features associated with the supernova are  $10,000 \text{ km s}^{-1}$  wide, so they remain fully resolved at  $R = 100$ . The lower resolution spectrum is shown twice for comparison, and key line features are identified. **Right:** Success rate for classifying supernovae from single epoch spectroscopy as a function of resolution using cross-correlation to a library of supernova templates.

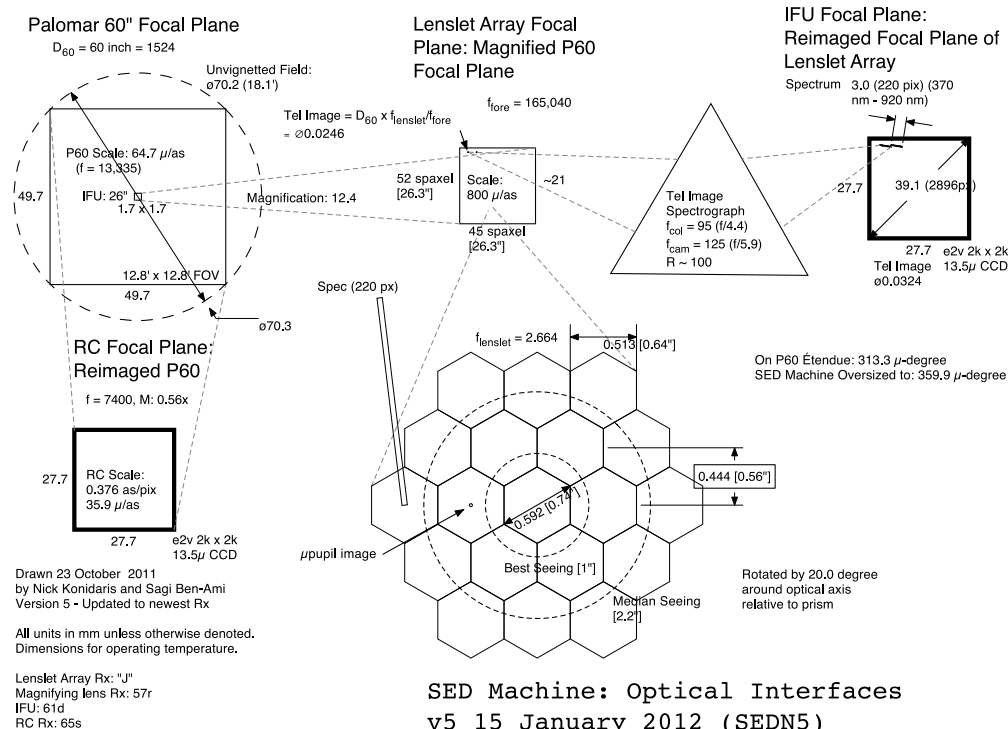


Figure 2. The SED Machine Optical Interfaces. The P60 focal plane is shared by the IFU spectrograph and the RC imager. The IFU has a  $26'' \times 26''$  FoV divided with hexagonal spaxels. Light from the reimaged pupils is dispersed by a constant resolution triple prism and refocused on a Princeton Instrument PIXIS 2048-Excelsion camera. The RC is a  $12.5' \times 12.5'$  imager with a FoV divided to 4 different bands. The RC also utilizes a Princeton Instrument PIXIS 2048 camera.

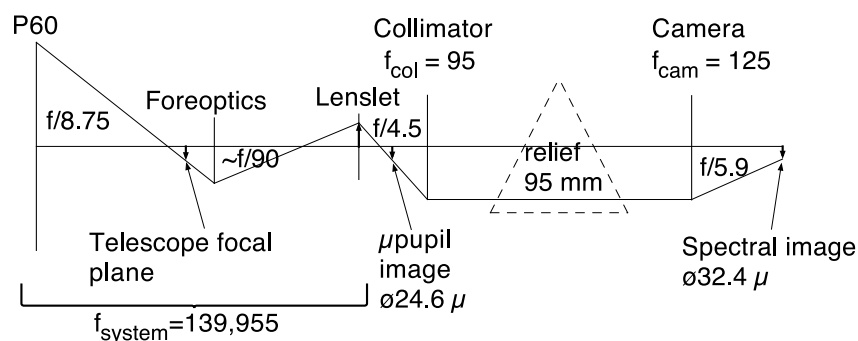


Figure 3. Paraxial layout of the IFU Spectrograph. Linear units in mm unless denoted otherwise. The dimensions  $f_{system}$ ,  $f_{col}$ ,  $f_{lenslet}$ , and  $f_{cam}$  refer to focal lengths.

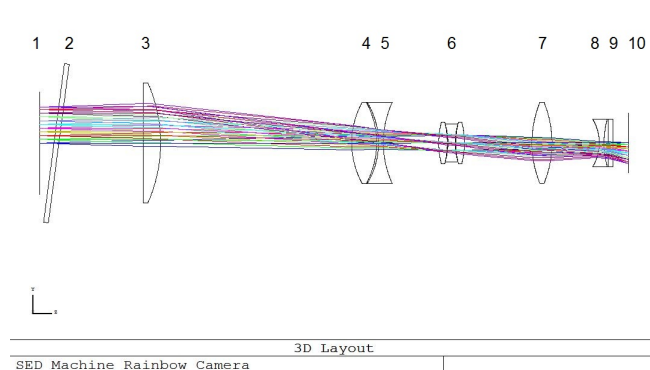


Figure 4. Rainbow Camera layout: (1) P60 focal plane, (2) Filters frame tilted by  $7.5^\circ$  to reduce ghost images, (3) Field Lens - Thorlabs LA4795, (4) Thorlabs LB4592, (5) Custom i-line glass lens, (6) Achromatic Triplet - Edmund Optics NT64838, (7) Thorlabs LB4553, (8) i-line glass field flattener, (9) Camera window, (10) RC image plane (CCD location).

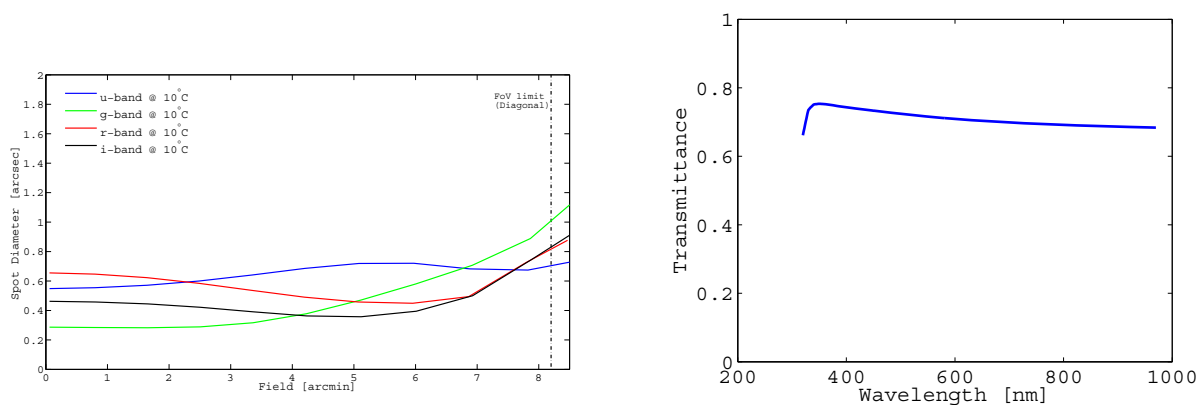


Figure 5. **Left:** RC performance at  $10^\circ\text{C}$ . The spot diameters are all below the seeing at the P60 telescope. **Right:** RC transmittance stands at  $\sim 75\%$  for all wavelengths of operation.

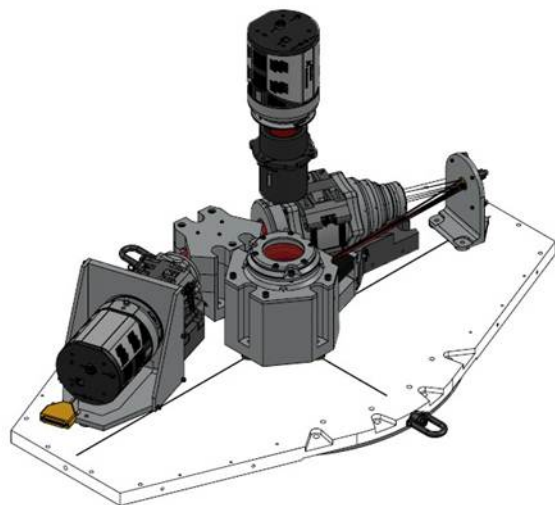


Figure 6. The SED machine layout.

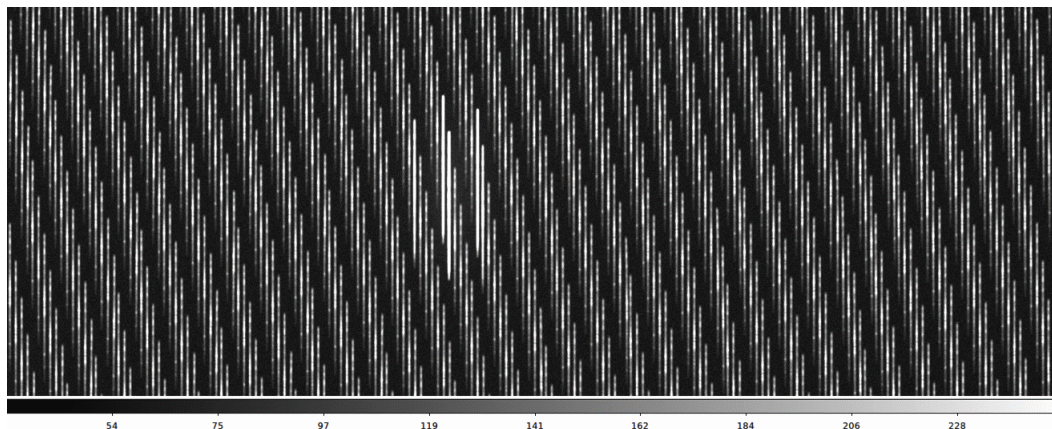


Figure 7. Data Simulator showing the spectral traces. A source is shown near the middle of the format. Most spectra show sky background.



## REFERENCES

- [1] Sweeney, D. W. 2006, Proceedings of the International Society for Optical Engineering, 6267
- [2] Katz, B., Budnik, R., & Waxman, E. 2010, Astrophysical Journal, 716, 781
- [3] Quimby, R. M., Kulkarni, S. R., Kasliwal, M. M., et al. 2011, Nature, 474, 487
- [4] Kasliwal, M. M., Kulkarni, S. R., Gal-Yam, A., et al. 2011, arXiv:1111.6109
- [5] Sari, R., Piran, T., & Narayan, R. 1998, Astrophysical Journal Letters, 497, L17
- [6] Greiner, J., Bornemann, W., Clemens, C., et al. 2008, Publications of the Astronomical Society of the Pacific, 120, 405
- [7] Bus, S. J., & Binzel, R. P. 2002, Icarus, 158, 146
- [8] Bacon, R., Adam, G., Baranne, A., et al. 1995, Astronomy and Astrophysics, Supplement, 113, 347
- [9] Lantz, B., Aldering, G., Antilogus, P., et al. 2004, Proceedings of the International Society for Optical Engineering, 5249, 146
- [10] Law, N. M., Kulkarni, S. R., Dekany, R. G., et al. 2009, Publications of the Astronomical Society of the Pacific, 121, 1395
- [11] Rau, A., Kulkarni, S. R., Law, N. M., et al. 2009, Publications of the Astronomical Society of the Pacific, 121, 1334
- [12] Bloom, J. S., Starr, D. L., Butler, N. R., et al. 2009, Bulletin of the American Astronomical Society, 41, #469.07
- [13] Lang, D., Hogg, D. W., Mierle, K., Blanton, M., & Roweis, S. 2010, Astronomical Journal, 139, 1782
- [14] Bertin, E., & Arnouts, S. 1996, Astronomy and Astrophysics, Supplement, 117, 393
- [15] Ritter, A., & Washuettl, A. 2004, Astronomische Nachrichten, 325, 663
- [16] Krige D. G, 1951, Master's thesis, 1951
- [17] Matheron, G., Economic Geology, 1963, 58, 1246
- [18] Ritter A., Diploma thesis, 2007
- [19] Piskunov, N. E., & Valenti, J. A. 2002, Astronomy and Astrophysics, 385, 1095